

## ESI Electronic Supplementary Information, ESI

### Can slow-moving ions explain hysteresis in the current-voltage curves of perovskite solar cells?

Giles Richardson,<sup>a</sup> Simon E. J. O’Kane,<sup>b</sup> Ralf G. Niemann<sup>c</sup>, Timo A. Peltola<sup>b</sup>, Jamie M. Foster<sup>d</sup>, Petra J. Cameron<sup>c</sup> and Alison B. Walker<sup>e</sup>

<sup>a</sup>Mathematical Sciences, University of Southampton, UK, <sup>b</sup>Department of Physics, University of Bath, UK, <sup>c</sup>Department of Chemistry, University of Bath, UK, <sup>d</sup>Department of Mathematics and Statistics, McMaster University, Hamilton, Canada, <sup>e</sup>Department of Physics, University of Bath, UK. E-mail: a.b.walker@bath.ac.uk

#### ESI Note 1: Drift-diffusion (DD) model for iodide vacancies

Figs. 3 and 4 in the main article compare the conduction band edge  $E_C(x,t)$  and the iodide vacancy density  $P(x,t)$  obtained via two different methods: the asymptotic method outlined in the main article and a numerical drift-diffusion method, which is outlined here. The drift-diffusion method is centred around solving the continuity equations

$$\frac{\partial P}{\partial t} + \frac{\partial F_p}{\partial x} = 0, \quad \text{where} \quad F_p = D_+ \left( \frac{P}{k_B T} \frac{\partial E_C}{\partial x} - \frac{\partial P}{\partial x} \right) \quad (1)$$

and Poisson’s equation of electrostatics

$$\frac{\partial^2 E_C}{\partial x^2} = \frac{q^2}{\epsilon_p} (P - N_0) \quad (2)$$

simultaneously, where  $F_p$  is the vacancy flux,  $k_B$  is the Boltzmann constant,  $T$  is absolute temperature (assumed here to be 298 K) and  $q$  is the electronic charge. Descriptions and values for  $\epsilon_p$  and  $D_+$  are given in Tables 1 and 2 of the main article respectively. Equations (1) and (2) are usually given in terms of the electrostatic potential  $\phi(x,t)$  as opposed to the conduction band edge  $E_C(x,t)$ . It is possible to switch between the two formulations by noting that  $E_C(x,t) = E_0 - q\phi(x,t)$ , where  $E_0$  is the energy relative to which  $E_C(x,t)$  is defined. For the purposes of this work  $E_0 = E_C(x,0) \forall x$ , *i.e.* the conduction band edge under flat band conditions.

#### ESI Note 2: Drift-diffusion (DD) model for electrons and holes

Equations (1) and (2) of this Note are the continuity equations for electrons and holes combined with the equations for the current densities in terms of their diffusion and drift components. The current-voltage,  $J$ - $V$ , curves are obtained by solving a one-dimensional transport model for the charge carriers (electrons and holes) within the perovskite ( $0 < x < b$ ). This takes the standard form

$$\frac{\partial p}{\partial t} + \frac{1}{q} \frac{\partial j_p}{\partial x} = G(x) - R(n,p), \quad \text{where} \quad j_p = q \hat{D}_p \left( \frac{p}{V_T} E_{bulk} - \frac{\partial p}{\partial x} \right), \quad (3)$$

$$\frac{\partial n}{\partial t} - \frac{1}{q} \frac{\partial j_n}{\partial x} = G(x) - R(n,p), \quad \text{where} \quad j_n = q \hat{D}_n \left( \frac{n}{V_T} E_{bulk} + \frac{\partial n}{\partial x} \right), \quad (4)$$

in which the variables:  $n$  and  $p$  denote electron and hole densities, respectively;  $j_n$  and  $j_p$  denote electron and hole currents, respectively; and  $E(x,t)$  denotes the electric field. The parameters  $\hat{D}_n$ ,  $\hat{D}_p$  and  $V_T$  are described in Table 1 of the main article. The latter, as discussed in the main article, is well-approximated, in the central region of the perovskite (away from the Debye layers) by  $E_{bulk}(t)$  as defined in equation (3) of the main article. The charge generation term  $G(x)$  is given by the Beer-Lambert law of light absorption which, since the light enters from the left of the device (through the  $\text{TiO}_2$  layer), has the form

$$G = F_{ph} \alpha \exp[-\alpha x], \quad (5)$$

where  $F_{ph}$  is the incident photon flux and  $\alpha$  is the light absorption coefficient of the perovskite. Charge carrier recombination is modelled by a Shockley-Read-Hall term of the form

$$R = \frac{np - n_i^2}{\tau_n n + \tau_p p}, \quad (6)$$

where  $n_i$  is the intrinsic carrier density. We have ignored the term  $n_i^2$  as we are always well away from equilibrium. Estimates for the electron and hole pseudo-lifetimes ( $\tau_n$  and  $\tau_p$ ) are given in Table 2 in the main article. The physical origin of the pseudo-lifetimes is given by<sup>1</sup>

$$\tau_n = \frac{1}{N_t v_{th} \sigma_p} \quad \text{and} \quad \tau_p = \frac{1}{N_t v_{th} \sigma_n}, \quad (7)$$

where  $N_t$  is the density of traps,  $v_{th}$  is the thermal velocity and  $\sigma_n$  and  $\sigma_p$  are the electron and hole capture cross-sections respectively. Crucially, the psuedo-lifetime of one carrier type is inversely proportional to the capture cross-section of the other type.

Since we believe that bulk recombination, rather than interfacial recombination, is the source of the hysteresis we neglect the effects of recombination via surface traps on the perovskite-TiO<sub>2</sub> and the perovskite-spiro interfaces and impose zero hole current on the former and zero electron current on the latter. It is assumed that the doping levels in the buffer layers are sufficiently high so that they are at the same potential as their respective contacts. It follows that the potentials at the perovskite-buffer layer interfaces are equal to the potentials at the respective contacts. The boundary conditions on (3)-(4) thus read

$$\left. \begin{array}{l} n = n_0 \\ j_p = 0 \end{array} \right\} \text{ on } x = 0, \quad \left. \begin{array}{l} p = p_0 \\ j_n = 0 \end{array} \right\} \text{ on } x = b. \quad (8)$$

Numerical solution to the carrier transport equations (3)-(8) proves difficult for the same reasons that the solution to the ionic one proves problematic, that is because of the presence of the narrow Debye layers adjacent to the edges of the perovskite (on  $x = 0$  and  $x = b$ ) over which the solutions to  $n$  and  $p$  vary extremely rapidly. This difficulty may be overcome by noting that there is minimal band bending within the Debye layers so that  $n$  and  $p$  vary exponentially (in the standard fashion) with the potential in these layers. It follows that the boundary conditions at the interfaces (8) can be replaced by the standard approximate ones

$$\left. \begin{array}{l} n = n_0 \exp\left(\frac{\mathbf{V}_-(t)}{V_T}\right) \\ j_p = 0 \end{array} \right\} \text{ on } x = 0^+, \quad \left. \begin{array}{l} p = p_0 \exp\left(-\frac{\mathbf{V}_+(t)}{V_T}\right) \\ j_n = 0 \end{array} \right\} \text{ on } x = b^-, \quad (9)$$

which hold on the interior of the respective Debye layers (denoted by  $x = 0^+$  and  $x = b^-$  to highlight the fact that these regions lie just inside the perovskite layer). Here  $\mathbf{V}_- = \mathbf{V}(-Q_+)$  is the potential drop from the TiO<sub>2</sub> interface (on  $x = 0$ ) to the interior of the adjacent Debye layer at  $x = 0^+$  and  $\mathbf{V}_+ = \mathbf{V}(Q_+)$  is the potential drop from the spiro interface (on  $x = b$ ) to the interior of the adjacent Debye layer at  $x = b^-$ . Solution of (3)-(4) is then made throughout the bulk region  $0^+ < x < b^-$  with the appropriate asymptotic expression for the electric field in the bulk, namely

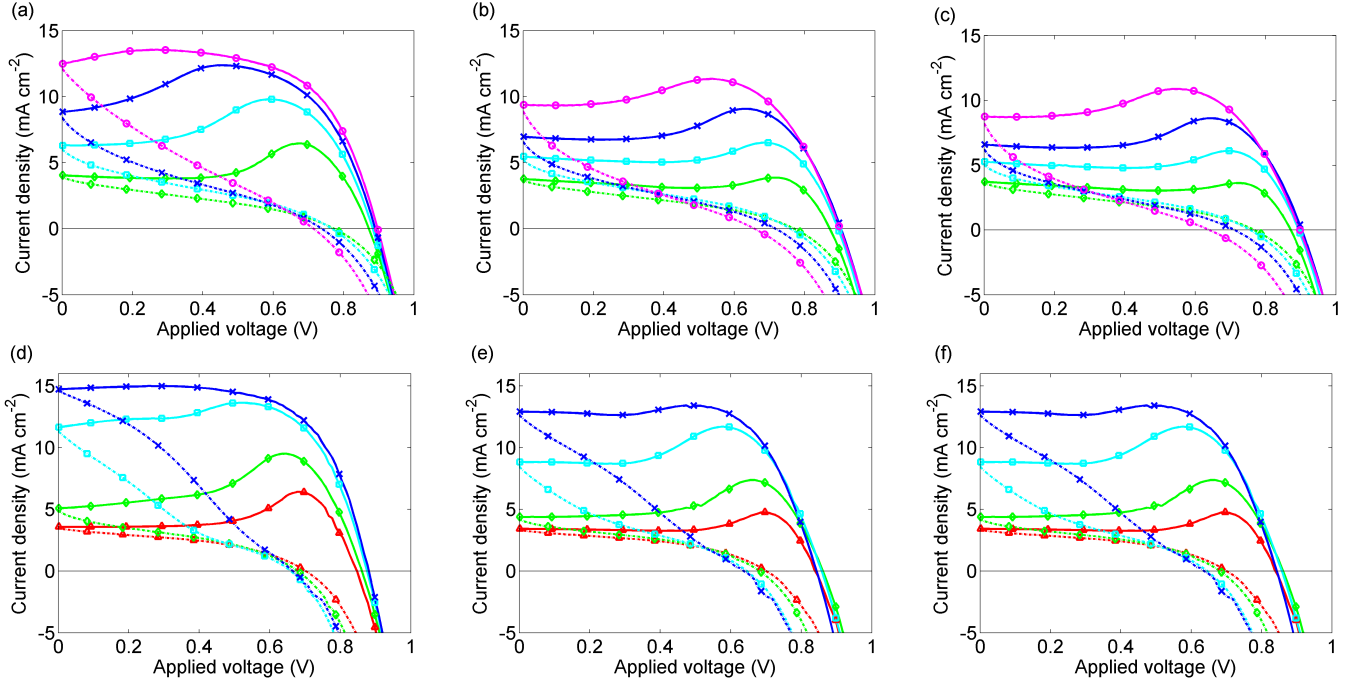
$$E = E_{bulk}(t) = \frac{V_{bi} - V(t) - \mathbf{V}(Q_+(t)) + \mathbf{V}(-Q_+(t))}{b}. \quad (10)$$

and used to calculate  $J(t) = j_n + j_p$  as the applied potential  $V(t)$  varies and hence to obtain  $J$ - $V$  curves for particular scanning profiles. The timescales used for generating these hysteresis curves are nearly always much greater than the timescale for relaxation of the charge carrier concentrations and consequently the error made in neglecting the time derivatives in (3)-(4) is negligible.

Here numerical solution of (3)-(4) and (9)-(10) is accomplished using the same package used for the ionic problem, namely Chebfun, because although the effects of the Debye layers have been accounted for using an asymptotic technique the problem is stiff (and therefore hard to resolve numerically) when  $E$  is large.

## References

- [1] S. Sze, *Physics of Semiconductor Devices, 2nd Edition*, John Wiley & Sons, New York, 2002.

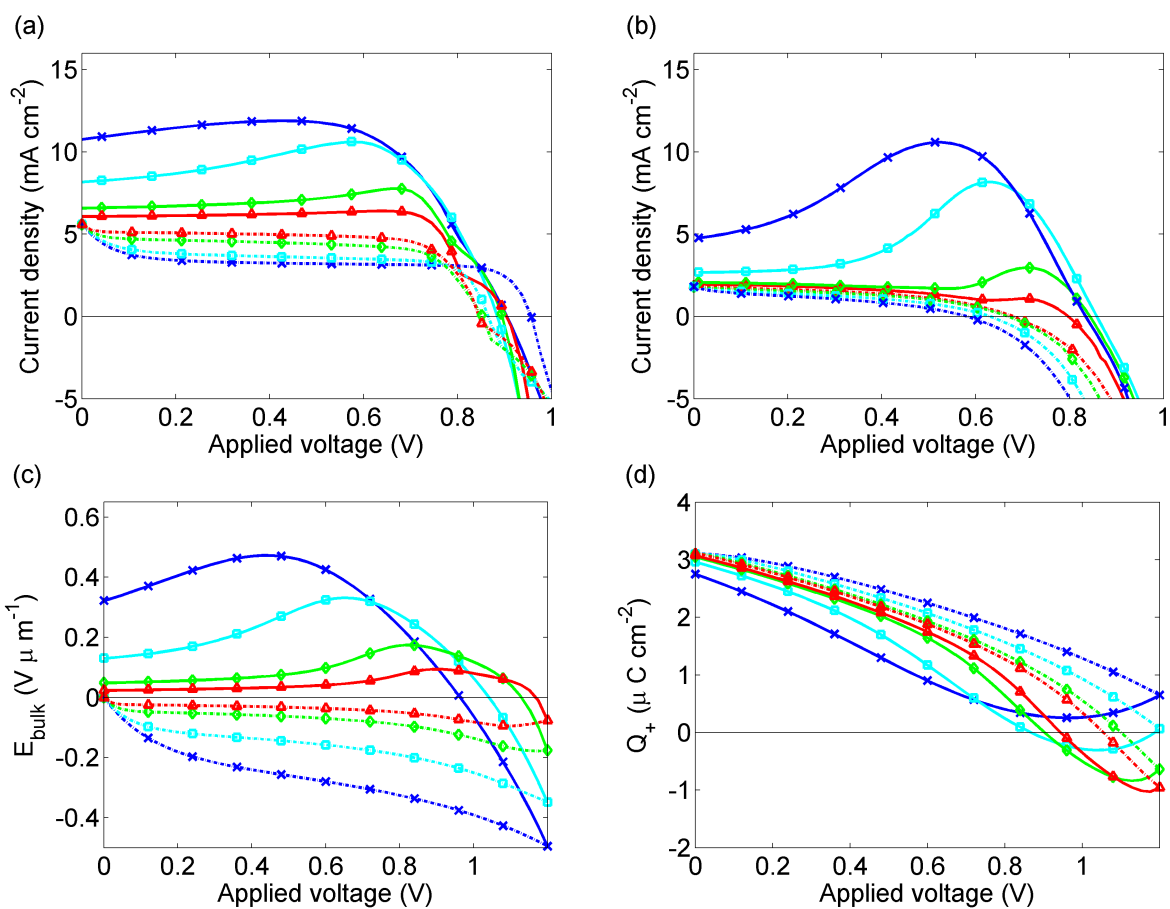


**ESI Fig. 1.**

Measured  $J$ - $V$  curves for cells 1 and 2 preconditioned for 5s at 1.2V. Cell 1: (a) first scan, (b) second scan, (c) third scan. Cell 2: (d) first scan, (e) second scan, (f) third scan. Solid lines show the 1.2 V to 0 V scan; broken lines show the 0V to 1.2 V scan. Scan rates are 1 V/s (magenta, circles), 500 mV/s (blue, crosses), 250 mV/s (cyan, filled squares), 100 mV/s (green, diamonds). For cell 2, we also show results for a scan rate of 50 mV/s (red, triangles)

### ESI Note 3: Preconditioning at short circuit

ESI Fig. 2 contains measurements (a) and simulations (b),(c),(d) of cell 2 for the case where the cell was preconditioned at short circuit as opposed to 1.2 V. For faster scans,  $Q_+$  at  $V \approx 1.2$  V in ESI Fig. 2 (d) for the 1.2 V to 0 V scan is larger for preconditioning at 0 V compared to  $Q_+$  where preconditioning is at 1.2 V shown in Fig. 8 (b) in the main article. This difference in  $Q_+$  has little effect on the current  $J$  predicted by the model due to inaccuracies in the diffusion currents when there is a large amount of electronic charge in the cell, as discussed in the main article. However, the measured currents differ significantly between the two preconditioning experiments even for the slow scans where  $Q_+$  is predicted to be similar for both types of preconditioning. It is possible that  $D_+$  has been overestimated so that the simulated  $I^-$  vacancies respond too quickly to changes in the voltage compared to in the experiments. Some degradation may have taken place during the measurement for preconditioning at 1.2 V, which were performed first, although we would not expect significant changes in cell output over this short period.



**ESI Fig. 2.**

$J-V$  curves, fields and accumulated ionic charge for the first scan of cell 2. Scan rates are  $500 \text{ mV s}^{-1}$  (blue),  $250 \text{ mV s}^{-1}$  (cyan),  $100 \text{ mV s}^{-1}$  (green) and  $50 \text{ mV s}^{-1}$  (red). Solid lines show the 1.2 V to 0 V scan dashed lines the 0V to 1.2V scan. Top panels:  $J-V$  curves with 5 s preconditioning at 0 V; (a) calculated, (b) measured. Bottom panels: (c) Electric field  $E_{\text{bulk}}$  between the Debye layers and (d) charge per unit area  $Q_+$  in the Debye layer next to the spiro. When  $E_{\text{bulk}} > 0$ , holes drift towards the spiro and electrons towards the  $\text{TiO}_2$ .